3.15 WAVEFORM GENERATOR

The purpose of the radar transmitter is to emit an RF signal having characteristics favorable for processing of similar signals reflected from a target. Transmitter performance in *RADGUNS* is simulated by generation of pulses at the radar's pulse repetition frequency (PRF). Each pulse has a zero rise time and the same amount of RF energy (amplitude). The transmitted waveform is characterized in the model by constant time values for pulse width (PW) and pulse repetition interval (PRI). Figure 3.15-1 shows a typical pattern, or train, of pulses and the time measurements used to simulate them. The carrier frequency (*f*) and wavelength (λ) values are defined for electromagnetic propagation at the speed of light by the following relationship:

$$c = f\lambda$$

where: *c* is the speed of light.

In addition, transmitter power or energy radiated by the antenna affects the amount of energy reflected by the target, which is evidenced in detection performance. Other waveform parameters affect tracking performance via synchronization with angle and range gates in the receiver.

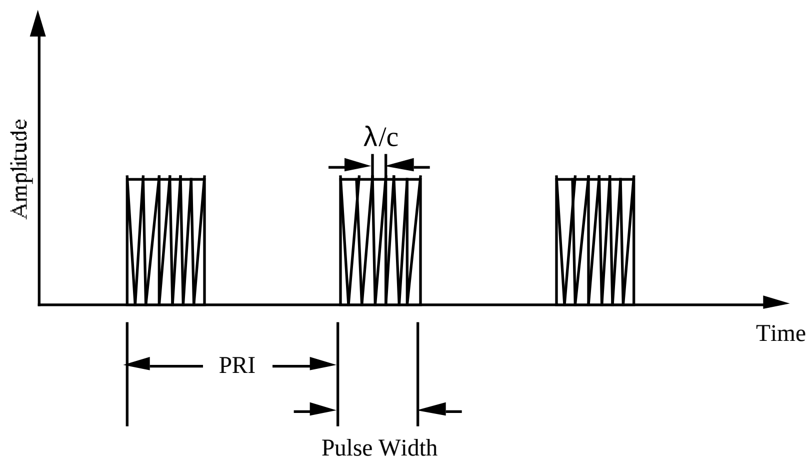

FIGURE 3.15-1. Typical *RADGUNS* Multiple Pulse Signal.

Data Items Required

Data Item		Accuracy	Sample Rate	Comments
3.1.1	Radar power	±1%	4 kHz	Limit to 10 s intervals
3.1.2	Pulse width	±2 ns	4 kHz	Limit to 10 s intervals
3.1.3	PRF/PRI	±10%	SV/T	
3.1.4	Detection time	±0.5 s	SV/T	
3.1.5	Tracking azimuth	±0.1 deg	10 Hz	
3.1.6	Tracking elevation	±0.1 deg	10 Hz	
3.1.7	Tracking range	±5 m	10 Hz	
3.1.8	Radar wavelength	±1%	SV/T	
3.1.9	Radar frequency	±1%	SV/T	

3.15.1 Power Sensitivity

3.15.1.1 Power Sensitivity Objectives and Procedures

RADGUNS uses the radar range equation to determine detection range:

$$R_{max} = \left[\frac{P_r G_r^2 \lambda^2 \sigma}{(4\pi)^3 LN(S/N)_{min}}\right]^{\frac{1}{4}}$$

where:

where:	R_{max}	=	maximum detection range
	P_r	=	transmitter power
	G_r	=	antenna gain factor
	λ	=	wavelength
	σ	=	RCS
	L	=	total loss factor
	N	=	noise
	S/N	=	signal-to-noise ratio

For any encounter, *RADGUNS* essentially reduces the above equation to the following form by maintaining several parameters as constants:

$$R_{max} = C(P_r \sigma)^{\frac{1}{4}}$$

where: $$C = \left[\frac{G_r^2 \lambda^2}{(4\pi)^3 LN(S/N)_{min}}\right]^{\frac{1}{4}}$$

Thus, detection range varies as the fourth root of the product of transmitter power and RCS.

The procedure used for analyzing model sensitivity to transmitter power settings was to record detection ranges when exercising *RADGUNS* under the following conditions:

a.	Model mode:	DETR
b.	Radar type:	RADR
c.	Target RCS:	0.1, 1.0, and 10.0 m^2
d.	Target altitude:	200 m
e.	Flight path:	LINEAR, 0 m offset
f.	Search radar:	Perfect cuing
g.	MTI:	Off
h.	Clutter:	None
i.	Multipath:	Disabled
j.	S/N:	14 dB (25.12)
k.	Radar power:	0.5, 0.95, 1.0, 1.05, 2.0, 3.0, and 4.0 x model baseline

3.15.1.2 Power Sensitivity Results

Figure 3.15-2 illustrates the effect of variations in radar power on detection range for three different target RCS values. Table 3.15-1 lists the specific data points illustrated in the figure.

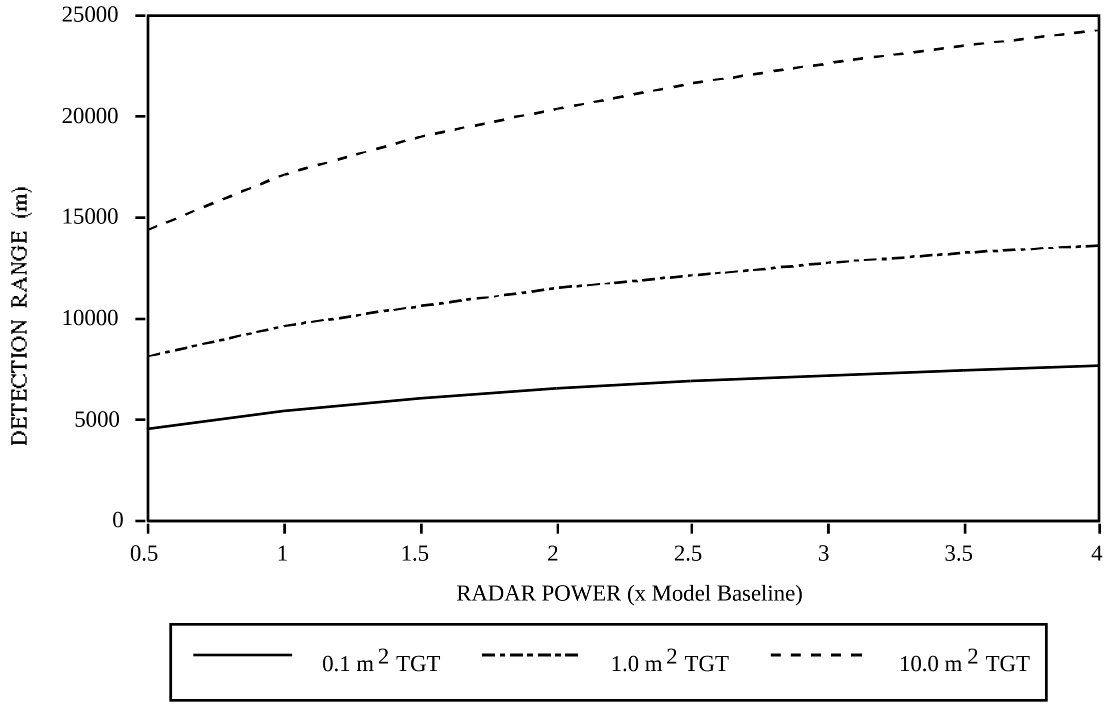

FIGURE 3.15-2. Transmitter Power Sensitivity.

TABLE 3.15-1. Detection Range as a Function of Radar Power and Target RCS.

Power Factor	**0.1-m^2 Tgt**	**1.0-m^2 Tgt**	**10.0-m^2 Tgt**
0.5	4523	8079	14,391
1.0	5387	9611	17,122
1.5	5966	10,641	18,953
2.0	6414	11,437	20,370
2.5	6784	12,096	21,541
3.0	7103	12,662	22,547
3.5	7383	13,161	23,435
4.0	7635	13,608	24,232

3.15.1.3 Power Sensitivity Conclusions

Detection range varies as the fourth root of transmitter power multiplied by target RCS. Variations in power can therefore be used to predict detection ranges for targets of known RCS, and these can be compared with values measured during testing. Given that recording a detection is a function of time, accuracy of detection range measurements will be a function of time resolution and target speed (the faster the target, the less accurate the range measurement).

3.15.2 Pulse Width Sensitivity

3.15.2.1 Pulse Width Sensitivity Objectives and Procedures

Angle and range tracking errors are sensitive to variations in pulse width. *RADGUNS* was executed under the following input parameter conditions:

a.	Model mode:	DETR
b.	Target RCS:	1.0 m^2
c.	Target altitude:	200 m
d.	Flight path:	LINEAR
e.	Radar type:	RAD1
f.	Pulse width:	0.50, 1.00, 1.50 nominal
g.	Output:	Angle and range tracking errors over time

3.15.2.2 Pulse Width Sensitivity Results

Figures 3.15-3, 3.15-4, and 3.15-5 show the effects of variation of pulse width on angle and range tracking errors. Pulse width changes affect angle tracking to a greater degree than range tracking.

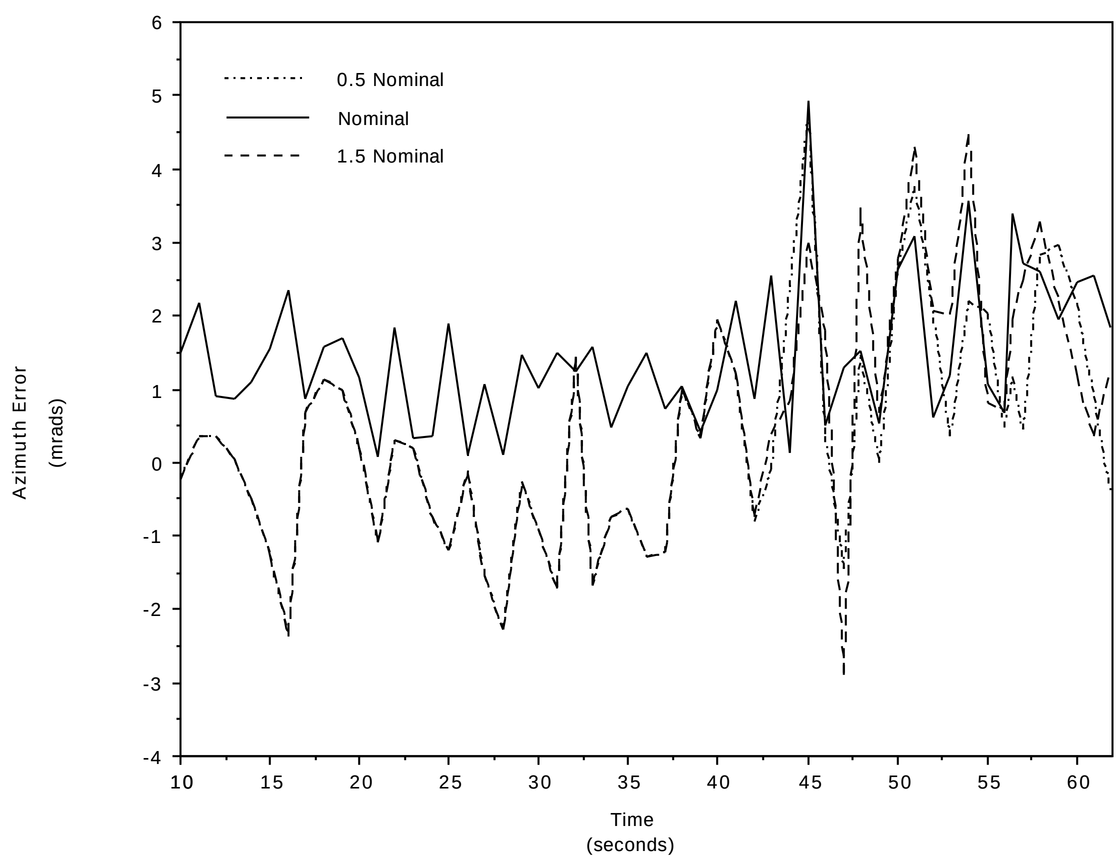

FIGURE 3.15-3. Azimuth Tracking Error as a Function of Pulse Width.

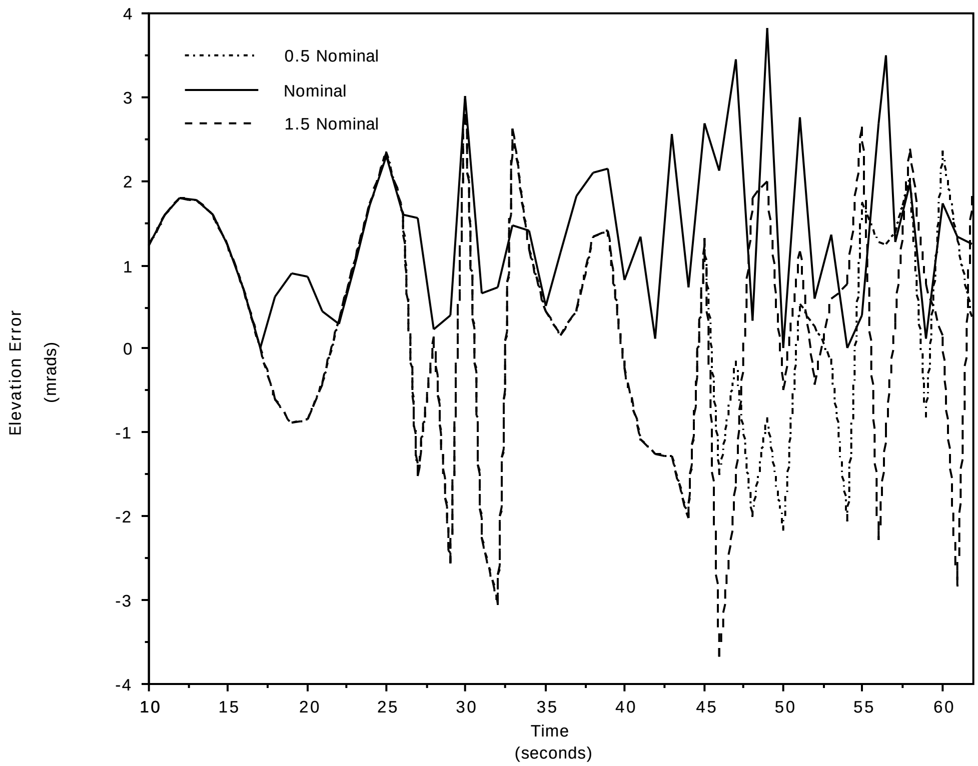

FIGURE 3.15-4. Elevation Tracking Error as a Function of Pulse Width.

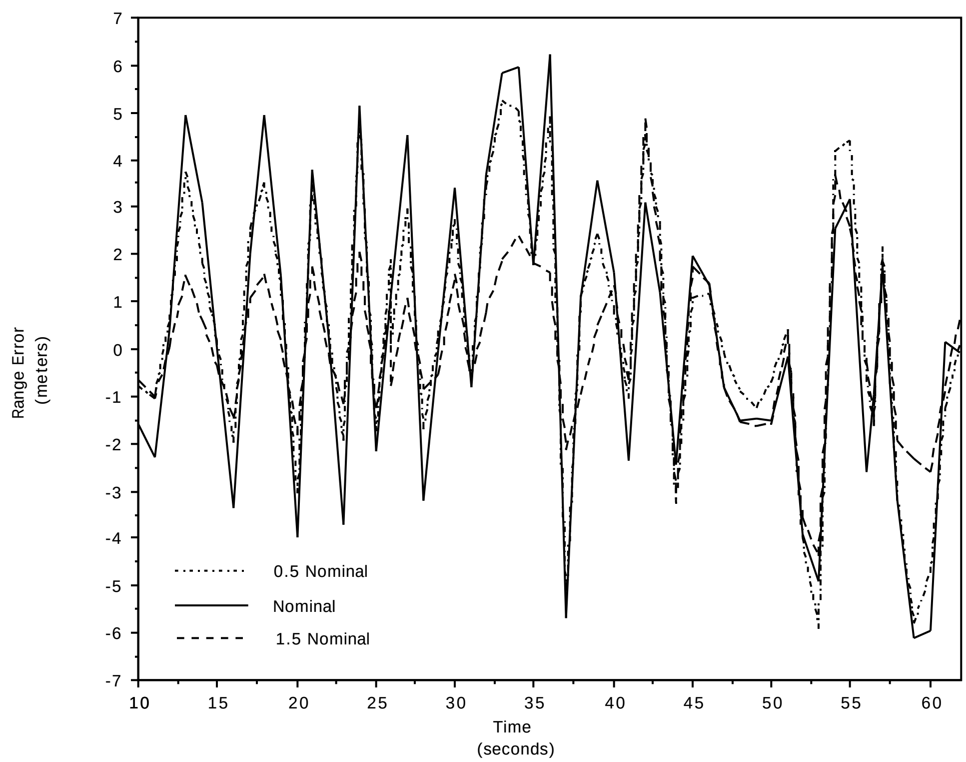

FIGURE 3.15-5. Range Tracking Error as a Function of Pulse Width.

3.15.2.3 Pulse Width Sensitivity Conclusions

For variations of ±50% of the nominal pulse width, errors are within the following:

Range tracking errors: ±5 m

Azimuth tracking errors: ±3 mrad

Elevation tracking errors: ±8 mrad

Table 3.15-2 summarizes the data analyzed for this functional element, along with the required parametric accuracies for functional element assessment.

TABLE 3.15-2. Pulse Width Parametric Requirements.

Tracking Parameter	**Pulse Width Variation (%)**	**Error Induced**	**Measurement Accuracy Required**
Azimuth	±50	±3 mrad	±1 mrad
Elevation	±50	±3 mrad	±1 mrad
Range	±50	±5 m	±2 m

3.15.3 Pulse Repetition Interval Sensitivity

3.15.3.1 Pulse Repetition Interval Sensitivity Objectives and Procedures

Angle and range tracking errors are sensitive to variations in the PRI because error signals derived from angle and range gates in the receiver are affected by shifts in the received waveform.

Effects of PRI were examined by running *RADGUNS* for the following conditions:

a. Model mode: SNGL/RADR
b. Target RCS: 10.0 m^2
c. Target altitude: 500 m
d. Flight path: LINEAR, 1000-m offset
e. Radar type: RAD1
f. PRI: Nominal
g. Output: Azimuth, elevation, and range tracking errors

Three simulated engagements were flown using the nominal and racking errors were then analyzed in three groups: azimuth, elevation, and range. Target velocity was 200 m/s, MTI off, clutter disabled, and multipath effects were not calculated.

Figure 3.15-6 compares azimuth tracking errors for the three different PRI values. All three curves show similar patterns of general shape and magnitude. To maintain consistency in analysis, the data were partitioned into two segments: ingress (time 60 to 94 s), and egress (time 104 to 138 s). This partitioning eliminated the adverse impact that biasing (positive errors on ingress, negative on egress) and crossover transients (in the vicinity of 100 s) would have on statistical measures. The parametric data for azimuth tracking errors during ingress are presented in Table 3.15-3. The key parameters are arithmetic mean ($\bar{X}$), standard deviation (σ), root-mean-square (RMS), and ingress average frequency (f_i).

DRAFT

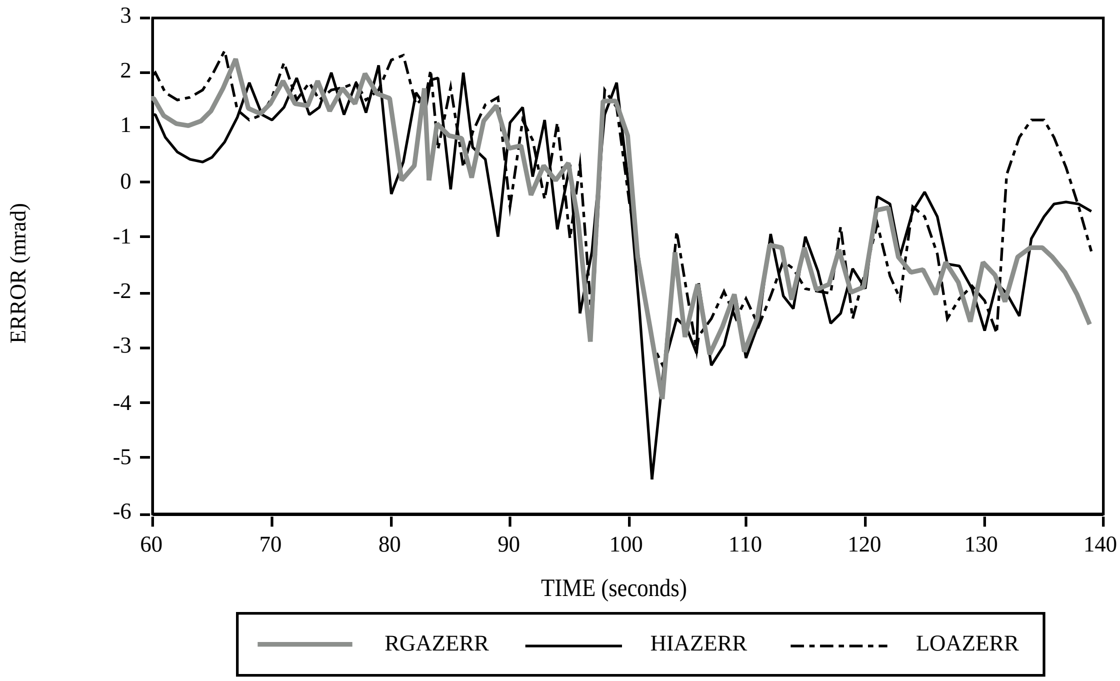

FIGURE 3.15-6. PRI Variation Azimuth Tracking Errors.

TABLE 3.15-3. Statistical Comparison of Azimuth Errors During Ingress.

Parameter	**Nominal**	**High PRI (Nom+10%)**	**Magnitude of Change**	**% Change**	**Low PRI (Nom-10%)**	**Magnitude of Change**	**% Change**
$\bar{X}$ *	1.0839	0.9939	0.0900	8.3	1.4268	0.3429	31.6
σ*	0.6194	0.7741	0.1547	25.0	0.6388	0.0194	3.1
RMS *	1.2442	1.2532	0.0090	0.7	1.5596	0.3154	25.4
f_i **	0.3235	0.2941	0.0294	9.1	0.2941	0.0294	9.1

* - Values in mrad
** - Values in Hz

Table 3.15-4 lists parametric data for azimuth errors during egress. In this table, f_e is the egress average frequency.

TABLE 3.15-4. Statistical Comparison of Azimuth Errors During Egress.

Parameter	**Nominal**	**High PRI (Nom+10%)**	**Magnitude of Change**	**% Change**	**Low PRI (Nom-10%)**	**Magnitude of Change**	**% Change**
$\bar{X}$ *			0.1065	6.0		0.3785	21.2
σ*	0.6225	0.9425	0.3200	51.4	1.1757	0.5532	88.9
RMS *	1.8877	1.9187	0.0310	1.6	1.8227	0.0650	3.4
f_e **	0.2941	0.2647	0.0294	10.0	0.2353	0.0588	20.0

* - Values in mrad
** - Values in Hz

DRAFT

Both tables contain several relatively large percentage of change values; the magnitude values, however, are very small. The highest magnitude of change, standard deviation for the low PRI egress, is only 0.5532 mrad, which is probably lower than most range systems can measure.

Elevation angle tracking errors are illustrated in Figure 3.15-7. Tables 3.15-5 and 3.15-6 list the parametric data for ingress and egress, respectively. The same general observations can be made for elevation tracking errors that were made for those of azimuth: Some of the percentages of change are relatively large but the magnitudes are small.

TABLE 3.15-5. Statistical Comparison of Elevation Errors During Ingress.

Parameter	Nominal	High PRI (Nom+10%)	Magnitude of Change	% Change	Low PRI (Nom-10%)	Magnitude of Change	% Change
$\bar{X}$ *	0.1999	0.3141	0.1142	57.1	0.3427	0.1428	71.4
σ*	1.0888	1.0466	0.0422	3.9	1.0338	0.0550	5.1
RMS *	1.0920	1.0787	0.0133	1.2	1.0754	0.0166	1.5
f_i **	0.2058	0.2353	0.0295	14.3	0.2058	0.0	0.0

* - Values in mrad
** - Values in Hz

TABLE 3.15-6. Statistical Comparison of Elevation Errors During Egress.

Parameter	Nominal	High PRI (Nom+10%)	Magnitude of Change	% Change	Low PRI (Nom-10%)	Magnitude of Change	% Change
$\bar{X}$ *	0.5492	0.3737	0.1755	32.0	0.1593	0.3899	71.0
σ*	1.5244	1.6111	0.0871	5.7	1.8231	0.2987	19.6
RMS *	1.6003	1.6320	0.0317	2.0	1.8047	0.2044	12.8
f_e **	0.2353	0.2647	0.0294	12.5	0.3235	0.0882	37.5

* - Values in mrad
** - Values in Hz

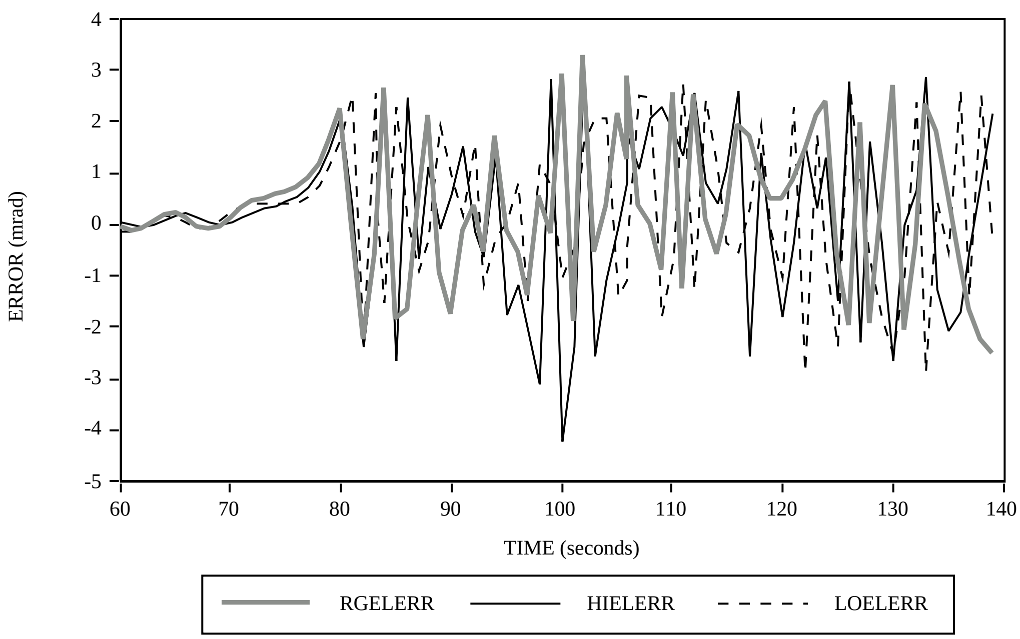

FIGURE 3.15-7. PRI Variation Elevation Tracking Errors.

Range tracking errors for the three different PRI values are illustrated in Figure 3.15-8. Tables 3.15-7 and 3.15-8 contain the ingress and egress statistical data for range tracking. As with azimuth and elevation, percentages of change are relatively significant for range tracking errors, but the magnitudes are very small. The largest, RMS for low PRI during egress, is less than 1 m.

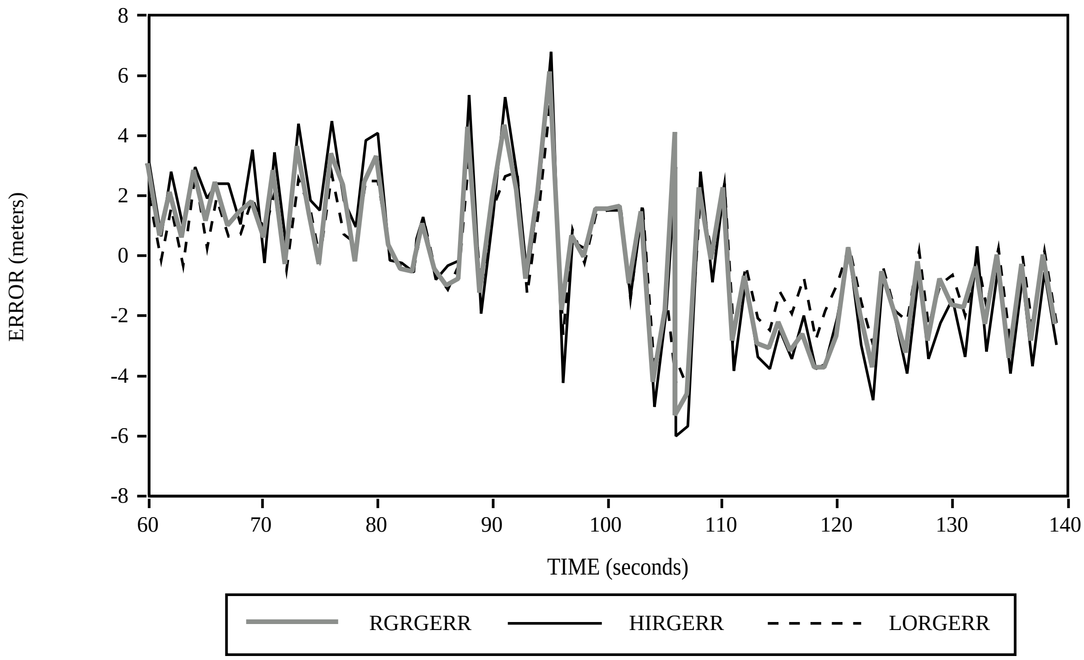

FIGURE 3.15-8. PRI Variation Range Tracking Errors.

TABLE 3.15-7. Statistical Comparison of Range Errors During Ingress.

Parameter	Nominal	High PRI (Nom+10%)	Magnitude of Change	% Change	Low PRI (Nom-10%)	Magnitude of Change	% Change
$\bar{X}$ *	1.2912	1.7318	0.4406	34.1	0.9765	0.3147	24.4
σ*	1.5876	1.8578	0.2702	17.0	1.3183	0.2693	17.0
RMS *	2.0292	2.5208	0.4916	24.2	1.6258	0.4034	19.9
f_i **	0.3235	0.3235	0.0	0.0	0.3235	0.0	0.0

* - Values in mrad
** - Values in Hz

TABLE 3.15-8. Statistical Comparison of Range Errors During Egress.

Parameter	Nominal	High PRI (Nom+10%)	Magnitude of Change	% Change	Low PRI (Nom-10%)	Magnitude of Change	% Change
$\bar{X}$ *			0.3930	22.4		0.3468	19.8
σ*	2.0348	2.2048	0.1700	8.4	1.5727	0.4621	22.7
RMS *	2.6655	3.0560	0.3905	14.7	2.0946	0.9614	36.1
f_i **	0.3824	0.3824	0.0	0.0	0.4118	0.0294	7.7

* - Values in mrad
** - Values in Hz

3.15.3.2 Pulse Repetition Interval Sensitivity Conclusions

Small variance (±10%) in PRI yielded extremely small changes in magnitude of tracking errors. Although some percentages of tracking error change were relatively high, the low magnitudes render these changes insignificant. This analysis concluded that for ±10% variance in PRI, no significant changes in tracking performance occurred.

3.15.4 Wavelength Sensitivity

3.15.4.1 Wavelength Sensitivity Objectives and Procedures

Wavelength and frequency vary inversely according to the equation for the speed of light in a vacuum:

$$c = \lambda f \qquad [3.15\text{-}1]$$

where: c = velocity of light (2.9979E8 m/s)
λ = wavelength (m)
f = frequency (Hz)

RADGUNS variables WLNTHA and WLNTHT correspond to carrier wavelengths of the acquisition and tracking radars, respectively. These parameters are constants for a particular radar type. Frequency is then computed within the model using Equation [3.15-1] in the form:

$$f = c / \lambda \qquad [3.15\text{-}2]$$

The basic radar equation is implemented in *RADGUNS* to calculate target echo power (S):

$$S = \frac{P_r G_r^2 \lambda^2 \sigma}{(4\pi)^3 R^4 L_t} \qquad [3.15\text{-}3]$$

where: P_r = radar transmitted power
G_r = antenna gain
λ = radar wavelength
σ = target RCS
R = range
L_t = total loss factor

RADGUNS models signal-to-noise ratio using target echo (S) as:

$$\frac{S}{N} = \frac{P_r G_r^2 \lambda^2 \sigma}{(4\pi)^3 R^4 L_t N} \qquad [3.15\text{-}4]$$

where the additional variable N is receiver noise power.

To analyze the effects of wavelength (and corresponding frequency) variation on model performance, three identical engagements were flown against a ZSU-23-4 with three different wavelengths. The simulation parameters used were:

a. Model mode: SNGL/PERC/RADR
b. Target RCS: 10 dBsm
c. TPA 6-sided 10 m^2
d. Target altitude: 200 m (clutter and multipath disabled)
e. Target speed 200 m/s
f. Flight path: LINEAR
g. Radar type: RAD1
h. MTI: Off
i. Guns: Disabled
j. Output: Target echo as a function of time

3.15.4.2 Wavelength Sensitivity Results

The tabulated statistical data in Table 3.15-9 for the three engagements indicate that a roughly 1:2 ratio exists between percentage of change in wavelength and percentage of change in the three general tendency parameters: mean, median, and standard deviation for target echo. This ratio is significant and points to a high degree of target echo sensitivity in the model. Figure 3.15-9 illustrates the echo results from the three runs.

TABLE 3.15-9. Target Echo Data.

Statistical Parameter	**Mean**	**Median**	**Standard Deviation**
RADGUNS Wavelength	1.71E-7 W	3.63E-8 W	2.55E-7 W
90% Wavelength	1.39E-7 W	2.93E-8 W	2.06E-7 W
% and Magnitude of Change	–18.7% 3.20E-8 W	–19.3% 7.00E-9 W	–19.2% 4.90E-8 W
110% Wavelength	2.07E-7 W	4.38E-8 W	3.08E-7 W
% and Magnitude of Change	+21.1% 3.60E-8 W	+20.7% 7.50E-9 W	+20.8% 5.30E-8 W

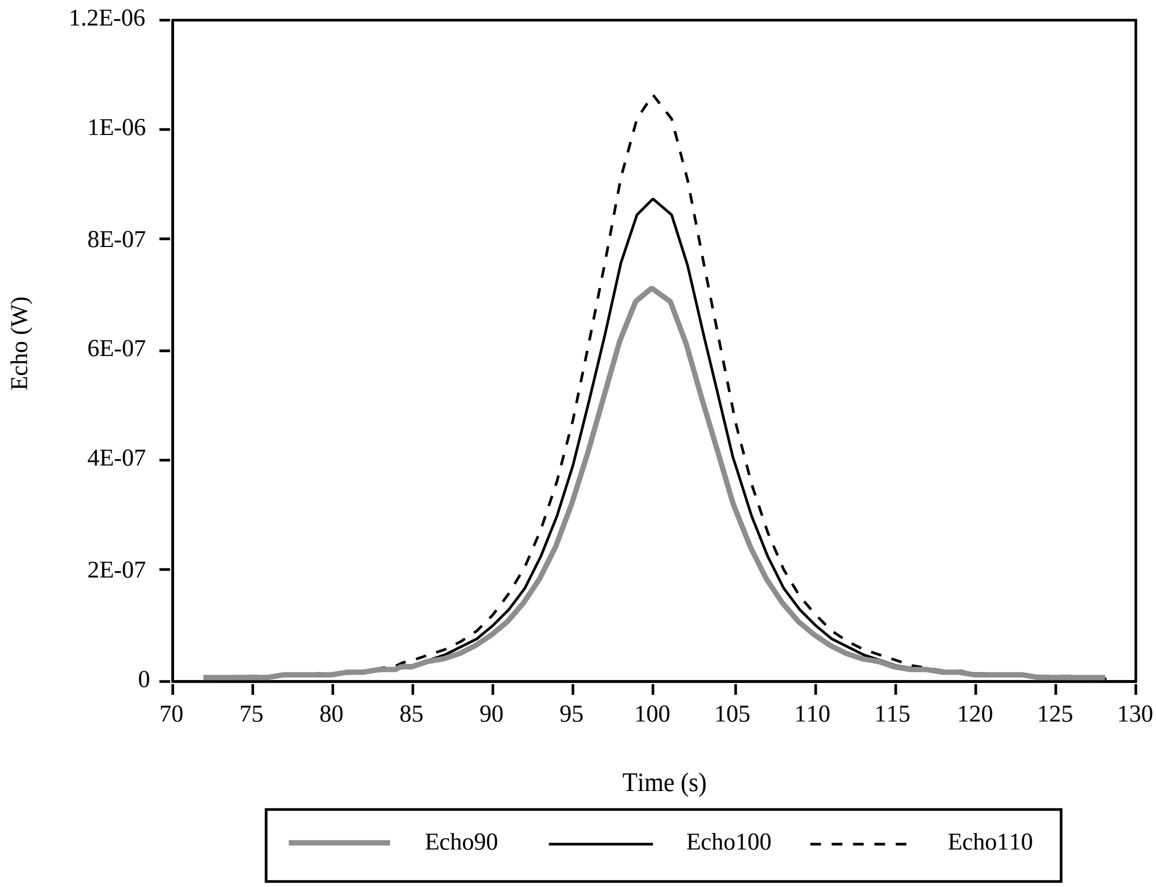

FIGURE 3.15-9. Target Echo Variance with Changes in Wavelength.

3.15.4.3 Wavelength Sensitivity Conclusions

For the three engagements studies, detection ranges were recorded as listed in Table 3.15-10. Here the variance ratio of percentage wavelength change to percentage of detection range change is 2:1.

TABLE 3.15-10. Detection Ranges Variance to Changes in Wavelength.

Case	**Detection Range (m)**	**% and Magnitude of Change (m)**
90% Wavelength	15,485	–5.4, 876
100% Wavelength	16,361	
110% Wavelength	17,198	–5.1, 837

Analysis indicates that wavelength changes affect detection range to a statistically significant degree. However, GUN DISH radar system detection ranges are typically much greater than the effective range of the guns and are therefore of only minor importance in *RADGUNS* engagement modeling.